Lab on a CD

Marc Madou, Jim Zoval, Guangyao Jia, Horacio Kido, Jitae Kim, and Nahui Kim

Department of Mechanical and Aerospace Engineering, University of California, Irvine, California 92697; email: jzoval@yahoo.com

Annu. Rev. Biomed. Eng. 2006. 8:601–28

First published online as a Review in Advance on May 2, 2006

The *Annual Review of Biomedical Engineering* is online at bioeng.annualreviews.org

doi: 10.1146/annurev.bioeng.8.061505.095758

1523-9829/06/0815-0601$20.00

Key Words

diagnostics, compact disc, centrifugal fluidics, microfluidics, BioMEMS

Abstract

In this paper, centrifuge-based microfluidic platforms are reviewed and compared with other popular microfluidic propulsion methods. The underlying physical principles of centrifugal pumping in microfluidic systems are presented and the various centrifuge fluidic functions, such as valving, decanting, calibration, mixing, metering, heating, sample splitting, and separation, are introduced. Those fluidic functions have been combined with analytical measurement techniques, such as optical imaging, absorbance, and fluorescence spectroscopy and mass spectrometry, to make the centrifugal platform a powerful solution for medical and clinical diagnostics and high throughput screening (HTS) in drug discovery. Applications of a compact disc (CD)-based centrifuge platform analyzed in this review include two-point calibration of an optode-based ion sensor, an automated immunoassay platform, multiple parallel screening assays, and cellular-based assays. The use of modified commercial CD drives for high-resolution optical imaging is discussed as well. From a broader perspective, we compare technical barriers involved in applying microfluidics for sensing and diagnostic use and applying such techniques to HTS. The latter poses less challenges and explains why HTS products based on a CD fluidic platform are already commercially available, whereas we might have to wait longer to see commercial CD-based diagnostics.

INTRODUCTION

Once it became apparent that individual chemical or biological sensors used in complex samples would not attain the hoped for sensitivity or selectivity, wide commercial use became severely hampered and sensor arrays and sensor instrumentation were proposed instead. It was projected that by using orthogonal sensor array elements (e.g., in electronic noses and tongues) selectivity would be improved dramatically (1). Researchers envisioned that instrumentation would reduce matrix complexities through filtration, separation, and concentration of the target compound, while at the same time ameliorate selectivity and sensitivity of the overall system by frequent recalibration and washing of the sensors. With microfluidics, the miniaturization of analytical equipment may potentially alleviate the shortcomings associated with large and expensive instrumentation through the reduction in reagent volumes; favorable scaling properties of several important instrument processes (basic theory of hydrodynamics and diffusion predicts faster heating and cooling and more efficient chromatographic and electrophoretic separations in miniaturized equipment); and batch-fabrication, which may enable low-cost, disposable instruments to be used once and then thrown away to prevent sample contamination (2). Micromachining (MEMS) might also allow cofabrication of many integrated functional instrument blocks. Tasks that are now performed in a series of conventional benchtop instruments could be combined into one unit, reducing labor and minimizing the risk of sample contamination.

Today it appears that sensor array development in electronic noses and tongues has slowed down because of lack of highly stable chemical and biological sensors: Too frequent recalibration of the sensors and relearning of the pattern recognition software is putting a damper on the original enthusiasm for this sensor approach. In the case of miniaturization of instrumentation through the application of microfluidics, progress was made in the development of platforms for high-throughput screening (HTS) as evidenced by new products introduced by, for example, Caliper and Tecan Boston (3, 4). In contrast, progress with miniaturized analytical equipment remained limited. Platforms have been developed for a limited amount of human and veterinary diagnostic tests that do not require complex fluidic design, for example, Abaxis (5). In this review, we are, in a narrow sense, summarizing the state of the art of compact disc (CD)-based microfluidics and, in a broader sense, we are comparing the technical barriers involved in applying microfluidics with sensing and diagnostic as opposed to applying such techniques to HTS. It is apparent that the former poses more severe technical challenges, and as a result, the promise of lab-on-a-chip has not been fulfilled yet.

WHY CENTRIFUGAL FORCE FOR FLUID PROPULSION?

There are various technologies for moving small quantities of fluids or suspended particles from reservoirs to mixing and reaction sites, to detectors, and eventually to waste or to the next instrument. Methods to accomplish this include syringe and peristaltic pumps, electrochemical bubble generation, acoustics, magnetics, DC and

Table 1 Comparison of microfluidics propulsion techniques

	Fluid propulsion mechanism			
Comparison	**Centrifuge**	**Pressure**	**Acoustic**	**Electrokinetic**
Valving solved?	Yes for liquids, no for vapor	Yes for liquids and vapor	No solution shown yet for liquid or vapor	Yes for liquids, no for vapor
Maturity	Products available	Products available	Research	Products available
Propulsion force influenced by	Density and viscosity	Generic	Generic	pH, ionic strength
Power source	Rotary motor	Pump, mechanical roller	5 to 40 V	10 kV
Materials	Plastics	Plastics	Piezoelectrics	Glass, plastics
Scaling	L^3	L^3	L^2	L^2
Flow rate	From less than 1 nl s^{-1} to greater than 100 μl s^{-1}	Very wide range (less than nl s^{-1} to liter s^{-1})	20 μl s^{-1}	0.001–1 μl sec^{-1}
General remarks	Inexpensive CD drive, mixing is easy, most samples possible (including cells). Better for diagnostics	Standard technique. Difficult to miniaturize and multiplex	Least mature of the four techniques. Might be too expensive. Better for smallest samples	Mixing difficult. High voltage source is dangerous and many parameters influence propulsion, better for smallest samples (HTS)

AC electrokinetics, centrifuge, etc. In **Table 1**, we compare four of the more important and promising fluid propulsion means (*6*). The pressure that mechanical pumps have to generate to propel fluids through capillaries is higher the narrower the conduit. Pressure and centripetal force are both volume-dependent forces, which scale as L^3 (in this case L is the characteristic length corresponding to the capillary diameter). Piezoelectric, electroosmotic, electrowetting, and electrohydrodynamic (EHD) pumping (the latter two are not shown in **Table 1**) all scale as surface forces (L^2), which represent more favorable scaling behavior in the microdomain (propulsion forces scaling with a lower power of the critical dimension become more attractive in the microdomain) and lend themselves better to pumping in smaller and longer channels. In principle, this should make pressure- and centrifuge-based systems less favorable, but other factors turn out to be more decisive; despite better scaling of the nonmechanical pumping approaches in **Table 1**, almost all biotechnology equipment today remains based on traditional external syringe or peristaltic pumps. The advantages of this approach are that it relies on well-developed, commercially available components, and that a very wide range of flow rates is attainable. Although integrated micromachined pumps based on two one-way valves may achieve a precise flow control on the order of 1 μl min^{-1} with fast response, high sensitivity, and negligible dead volume, these pumps generate only modest flow rates and low pressures, and they consume a large amount of chip area and considerable power.

Acoustic streaming is a constant (DC) fluid motion induced by an oscillating sound field at a solid/fluid boundary. A disposable fluidic manifold with capillary flow channels can simply be laid on top of the acoustic pump network in the reader instrument. The method is considerably more complex to implement than electroosmosis (see next section), but the insensitivity of acoustic streaming to the chemical nature of the fluids inside the fluidic channels and its ability to mix fluids make it a potentially viable approach. A typical flow rate measured for water in a small metal pipe lying on a piezoelectric plate is 0.02 cc s^{-1} at 40 V, peak to peak (7). Today acoustic streaming as a propulsion mechanism remains in the research stage.

Electroosmotic pumping (DC electrokinetics) in a capillary does not involve any moving parts and is easily implemented. All that is needed is a metal electrode in some type of a reservoir at each end of a small flow channel. Typical electroosmotic flow velocities are on the order of 1 mm s^{-1}, with a 1200 V cm^{-1} applied electric field. For example, in free-flow capillary electrophoresis work by Jorgenson (8), electroosmotic flow of 1.7 mm s^{-1} was reported. This is fast enough for most analytical purposes. Harrison et al. (9) achieved electroosmotic pumping with flow rates up to 1 cm s^{-1} in 20 μm capillaries that were micromachined in glass. They also demonstrated the injection, mixing, and reaction of fluids in a manifold of micromachined flow channels without the use of valves. The key aspect for tight valving of liquids at intersecting capillaries in such a manifold is the suppression of convective and diffusion effects. The authors demonstrated that these effects could be controlled by appropriate application of voltages to intersecting channels simultaneously. Some disadvantages of electroosmosis are the required high voltage (1–30 kV power supply) and direct electrical-to-fluid contact with resulting sensitivity of flow rate to the charge of the capillary wall and to the ionic strength and pH of the solution. It is consequently more difficult to make it into a generic propulsion method. For example, liquids with high ionic strength cause excessive Joule heating; it is therefore difficult or impossible to pump biological fluids such as blood and urine.

Using a rotating disc, centrifugal pumping provides flow rates ranging from less than 10 nl s^{-1} to greater than 100 μl s^{-1} depending on disc geometry, rotational rate (RPM), and fluid properties (see **Figure 1**) (10). Pumping is relatively insensitive to physicochemical properties such as pH, ionic strength, or chemical composition (in contrast to AC and DC electrokinetic means of pumping). Aqueous solutions, solvents (e.g., DMSO), surfactants, and biological fluids (blood, milk, and urine) have all been pumped successfully. Fluid gating, as we describe in more detail below, is accomplished using "capillary" valves in which capillary forces pin fluids at an enlargement in a channel until rotationally induced pressure is sufficient to overcome the capillary pressure (at the so-called burst frequency) or by hydrophobic methods. Because the types and the amounts of fluids one can pump on a centrifugal platform span a greater dynamic range than for electrokinetic and acoustic pumps, this approach seems more amenable to sample preparation tasks than electrokinetic and acoustic approaches. Moreover, miniaturization and multiplexing are quite easily implemented. A whole range of fluidic functions, including valving, decanting,

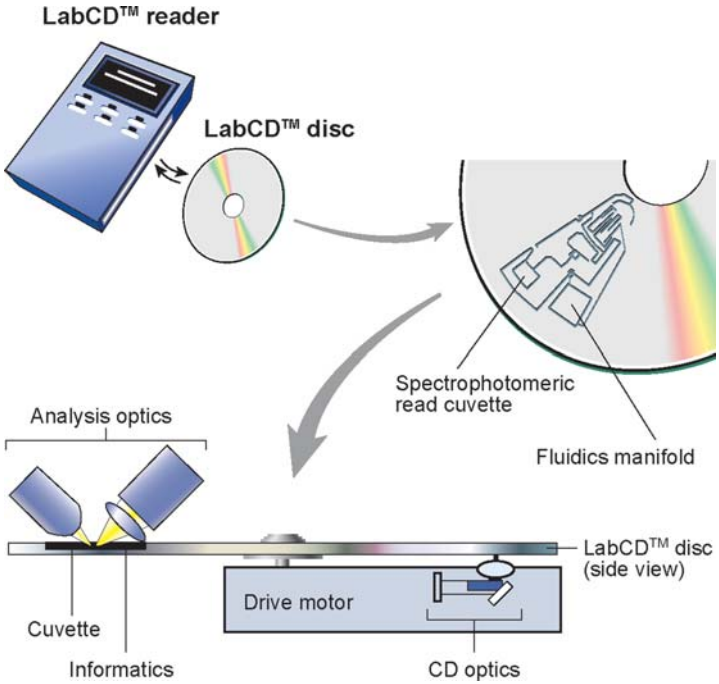

Figure 1

LabCD™ instrument and disposable disc. Here, the analytical result is obtained through reflection spectrophotometry.

calibration, mixing, metering, sample splitting, and separation, can be implemented on this platform, and analytical measurements may be electrochemical, fluorescent, or absorption based and informatics embedded on the same disc could provide test-specific information.

A most important deciding factor in choosing a fluidic system is the ease of implementing valves; the method that most elegantly solves the valving issue is already commercially accepted, even if the scaling is not the most favorable, namely, in the use of traditional pumps. In traditional pumps, two one-way valves form a barrier for both liquids and vapors. In the case of the microcentrifuge, valving is accomplished by varying rotation speed and capillary diameter. Thus, there is no real physical valve required for stopping water flow, but as in the case of acoustic and electrokinetic pumping, there is no simple means to stop vapors from spreading over the whole fluidic platform. If liquids need to be stored for a long time on the disposable component, as often is the case for use in sensing and diagnostics, valves must be barriers for both liquid and vapor. Some timid attempts at implementing vapor barriers on the CD are reported in this review.

From the preceding comparison of fluidic propulsion methods for sensing and diagnostic applications, centrifugation in fluidic channels and reservoirs crafted in a CD-like plastic substrate, as shown in **Figure 1**, constitutes an attractive fluidic platform.

COMPACT DISC OR MICRO-CENTRIFUGE FLUIDICS

How it Works

CD fluid propulsion is achieved through centrifugally induced pressure and depends on rotation rate, geometry and location of channels and reservoirs, and fluid properties. Madou et al. (11) and Duffy et al. (10) characterized the flow rate of aqueous solutions in fluidic CD structures and compared the results with simple centrifuge theory. The average velocity of the liquid (U) from centrifugal theory is given as

$$U = D_h^2 \rho \omega^2 \bar{r} \Delta r / 32 \mu L, \quad (1)$$

and the volumetric flow rate (Q) as

$$Q = UA, \quad (2)$$

where D_h is the hydraulic diameter of the channel (defined as 4A/P, where A is the cross-sectional area and P is the wetted perimeter of the channel), ρ is the density of the liquid, ω is the angular velocity of the CD, $\bar{r}$ is the average distance of the liquid in the channels to the center of the disc, Δr is the radial extent of the fluid, μ is the viscosity of the solution, and L is the length of the liquid in the capillary channel (see also **Figure 2*a***). Flow rates, ranging from 5 nl s^{-1} to >0.1 ml s^{-1}, have been achieved by various combinations of rotational speeds (from 400 to 1600 rpm), channel widths (20–500 μm), and channel depths (16–340 μm). The experimental flow rates were compared with rates predicted by the theoretical

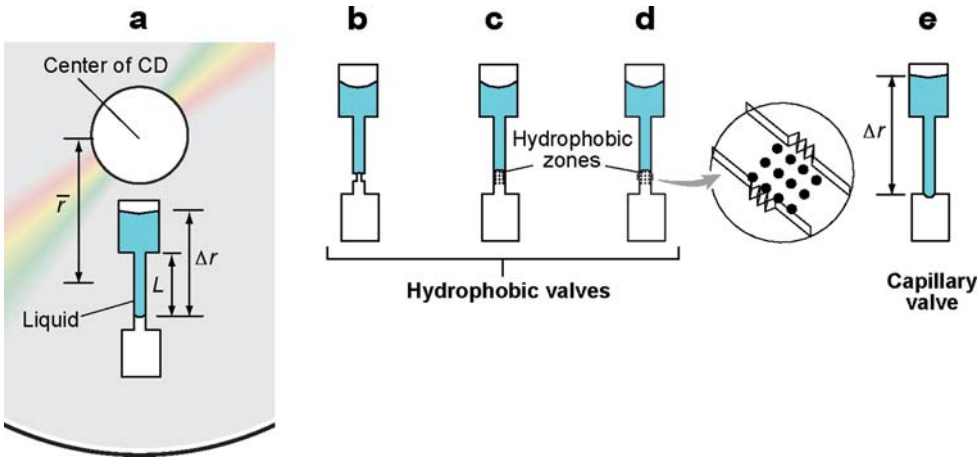

Figure 2

Schematic illustrations for the description of CD microfluidics. (*a*) Two reservoirs connected by a microfluidic chamber. (*b*) Hydrophobic valve made by a constriction in a chamber made of hydrophobic material. (*c*) Hydrophobic valve made by the application of hydrophobic material to a zone in the channel. (*d*) Hydrophobic channel made by the application of hydrophobic material to a zone in a channel made with structured vertical walls (*see inset*). (*e*) Capillary valve made by a sudden expansion in channel diameter, such as when a channel meets a reservoir.

model and exhibited an 18.5% coefficient of variation. The authors note that experimental errors in measuring the highest and lowest flow rates made for the largest contribution to this coefficient of variation. The absence of systematic deviation from theory validates the model for describing flow in microfluidic channels under centripetal force. Duffy et al. (10) measured flow rates of water, plasma, bovine blood, three concentrations of hematocrit, urine, dimethyl sulfoxide (DMSO), and PCR products and reported that centrifugal pumping is relatively insensitive to such physiochemical properties as ionic strength, pH, conductivity, and the presence of various analytes, noting good agreement between experiment and theory for all the liquids.

Some Simple Fluidic Function Demonstrated on a CD

Mixing of fluid. In the work by Madou et al. (11) and Duffy et al. (10), different means to mix liquids were designed, implemented, and tested. Observations of flow velocities in narrow channels on the CD enabled Reynolds numbers (R_e) calculations establishing that the flow remained laminar in all cases. Even in the largest fluidic channels tested, R_e was <100, well below the transition regime from laminar to turbulent flow ($R_e \sim 2300$) (12). The laminar flow condition necessitates mixing by simple diffusion or by creating special features on the CD that do enable advection or turbulence. In one scenario, fluidic diffusional mixing was implemented by emptying two microfluidic channels together into a single long meandering fluidic channel. Proper design of channel length and reagent reservoirs allowed for stoichiometric mixing in the meandering channel by maintaining equal flow rates of the two streams joining into the mixing channel. Concentration profiles may be calculated from the diffusion rates of the reagents and the time required for the liquids to flow through the tortuous path. Mixing can also be achieved by chaotic advection (6). Chaotic advection is a result of the rapid distortion and elongation of the fluid/fluid interface, increasing the interfacial area where diffusion occurs, which increases the mean values of the diffusion gradients that drive the diffusion process. One may call this process an enhanced diffusional process. In addition to simple and enhanced diffusional processes, one can create turbulence on the CD by emptying two narrow streams to be mixed into a common chamber. The streams violently splash against a common chamber wall causing their effective mixing (no continuity of the liquid columns is required on the CD, as opposed to the case of electrokinetics platforms where a broken-up liquid column would cause a voltage overload).

Valving. Valving is a most important function in any type of fluidic platform. Both hydrophobic and capillary valves have been integrated into the CD platform (10, 11, 13–23). Hydrophobic valves feature an abrupt decrease in the hydrophobic channel cross-section, i.e., a hydrophobic surface prevents further fluid flow (**Figure 2*b–d***). In contrast, in capillary valves (**Figure 2*e***), liquid flow is stopped by a capillary pressure barrier at junctions where the channel diameter suddenly expands.

Hydrophobic valving. The pressure drop in a channel with laminar flow is given by the Hagen-Poiseuille equation (12):

$$\Delta P = \frac{12 L \mu Q}{w h^3}, \tag{3}$$

where L is the microchannel length, μ is the dynamic viscosity, Q is the flow rate, and w and h are the channel width and height. The required pressure to overcome a sudden narrowing in a rectangular channel is given by the literature (6):

$$\Delta P = 2\sigma_l \cos(\theta_c)\left[\left(\frac{1}{w_1}\right) + \left(\frac{1}{h_1}\right)\right] - \left[\left(\frac{1}{w_2}\right) + \left(\frac{1}{h_2}\right)\right], \tag{4}$$

where σ_1 is the liquid's surface tension, θ_c is the contact angle, w_1 and h_1 are the width and height of the channel before the restriction, respectively, and w_2 and h_2 are the width and height after the restriction, respectively. In hydrophobic valving, for liquid to move beyond these pressure barriers, the CD must be rotated above a critical speed, at which point the centripetal forces exerted on the liquid column overcome the pressure needed to move past the valve.

Ekstrand et al. (13) used hydrophobic valving on a CD to control discrete sample volumes in the nanoliter range with centripetal force. Capillary forces draw liquid into the fluidic channel until there is a change in the surface properties at the hydrophobic valve region. The valving was implemented as described schematically in **Figure 2*c***. Tiensuu et al. (14) introduced localized hydrophobic areas in CD microfluidic channels by ink-jet printing of hydrophobic polymers onto hydrophilic channels. In this work, hydrophobic lines were printed onto the bottom wall of channels with both unstructured (**Figure 2*c***) and structured **Figure 2*d***) vertical channel walls. Several channel width-to-depth ratios were investigated. The CDs were made by injection molding of polycarbonate. The CDs were subsequently rendered hydrophilic by oxygen plasma treatment, and then ink-jet printing was used for the introduction of the hydrophobic polymeric material at the valve position. The parts were capped with Polydimethylsilxane (PDMS) to form the fourth wall of the channel. In testing of nonstructured channels (without saw-tooth pattern), there were no valve failures for 300- and 500-μm-wide channels, but there were some failures for the 100 μm channels; however, in structured vertical walls (with saw-tooth patterns), there were no valve failures. The authors attributed the better results of the structured vertical walls to both the favorable distribution of hydrophobic polymer within the channel and the sharper sidewall geometry to be wetted (the side walls are hydrophilic because the printed hydrophobic material is only on the bottom of the channel) compared with the nonstructured vertical channel walls.

Capillary valving. Capillary valves have been implemented frequently on CD fluidic platforms (10, 11, 15–18, 21, 22). The physical principle involved is based on the surface tension, which develops when the cross section of a hydrophilic capillary expands abruptly, as illustrated in **Figure 2*e***. As shown in this figure, a capillary channel connects two reservoirs, and the top reservoir (the one closest to the center of the CD) and the connecting capillary is filled with liquid. For capillaries with axisymetric cross sections, the maximum pressure at the capillary barrier expressed

in terms of the interfacial free energy (16) is given by

$$P_{cb} = 4\gamma_{al} \sin\theta_c / \mathrm{D}_h, \tag{5}$$

where γ_{al} is the surface energy per unit area of the liquid-air interface, θ_c is the equilibrium contact angle, and D_h is the hydraulic diameter. Assuming low liquid velocities, the flow dynamics may be modeled by balancing the centripetal force and the capillary barrier pressure (see Equation 5). The liquid pressure at the meniscus, from the centripetal force acting on the liquid, can be described as follows:

$$P_m = \rho\omega^2 \bar{r} \Delta r, \tag{6}$$

where ρ is the density of the liquid, ω is the angular velocity, $\bar{r}$ is the average distance from the liquid element to the center of the CD, and Δr is the radial length of the liquid sample (**Figure 2*a*, *e***). Liquid will not pass a capillary valve as long as the pressure at the meniscus (P_m) is less than or equal to the capillary barrier pressure (P_{cb}). Zeng and coworkers (16) named the point at which P_m equals P_{cb} the critical burst condition. The rotational frequency at which it occurs, they called the burst frequency. Experimental values of critical burst frequencies versus channel geometry, for rectangular cross sections over a range of channel sizes, show good agreement with simulation over the entire range of diameters studied. Because these simulations did not assume an axisymetric capillary with a circular contact line and a diameter D_h, the meniscus contact line may be a complex shape. Burst frequencies were shown to be cross-section dependent for equal hydraulic diameters. The theoretical burst frequency equation was modified as follows to account for variation of channel cross section:

$$\rho\omega^2 \bar{r} \Delta r < 4\gamma_{al} \sin\theta_c / (D_h)^n, \tag{7}$$

where $\mathrm{n} = 1.08$ for an equilateral triangular cross section and $\mathrm{n} = 1.14$ for a rectangular cross section. For "pipe flow" (circular cross section), an additional term is used in the burst frequency expression:

$$\rho\omega^2 \bar{r} \Delta r < 4\gamma_{al} \sin\theta_c / (D_h) + \gamma_{al} \sin\theta_c (1/\mathrm{D}_h - 1/\mathrm{D}_0), \tag{8}$$

where the empirically determined constant $\mathrm{D}_0 = 40$ μm. The physical reason for the additional "pipe flow" term, used to get a fit to the simulation results, is not well understood at this time.

Duffy et al. (10) modeled capillary valving by balancing the pressure induced by the centripetal force ($\rho\omega^2 \bar{r} \Delta r$) at the exit of the capillary with the pressure inside the liquid droplet being formed at the capillary outlet and the pressure required to wet the chamber beyond the valve. The pressure inside a droplet is given by the Young-Laplace equation (24):

$$\Delta \mathrm{P} = \gamma(1/\mathrm{R}_1 + 1/\mathrm{R}_2), \tag{9}$$

where γ is the surface tension of the liquid and R_1 and R_2 are the meniscus radii of curvature in the x and y dimensions of the capillary cross section, respectively. In the case of small circular capillary cross sections with spherical droplet shapes,

$R_1 = R_2 \cong$ channel cross section radius, and Equation 9 can be rewritten as

$$\Delta P = 4\gamma / D_h. \tag{10}$$

On this basis, Duffy et al. (10) derived a simplified expression for the critical burst frequency (ω_c):

$$\rho\omega_c^2 \bar{r}\Delta r = a(4\gamma / D_h) + b, \tag{11}$$

with the first term on the right representing the pressure inside the liquid droplet being formed at the capillary outlet scaled by a factor a (for nonspherical droplet shapes) and the second term on the right, b, representing the pressure required to wet the chamber beyond the valve. The b term depends on the geometry of the chamber to be filled and the wettability of its walls.

A plot of the centripetal pressure ($\rho\omega_c^2 \bar{r}\Delta r$) at which the burst occurs verses $1/D_h$ was linear, as expected from Equation 11, with a 4.3% coefficient of variation. The authors note a potential limitation with capillary valves owing to the fact that liquids with low surface tension tend to wet the walls of the chamber at the capillary valve opening, resulting in the inability to gate the flow. The b term in Equation 11 is beneficial in gating flow unless the surface walls at the abrupt enlargement of the capillary valve are so hydrophilic that the liquid is drawn past the valve and into the reservoir.

Madou et al. (17, 18) have designed a CD to sequentially valve fluids through a monotonic increase of rotational rate with progressively higher "burst" frequencies. The CD, shown in **Figure 3**, was designed to carry out an assay for ions based on an optode-based detection scheme. The CD design employed five serial capillary valves opening at different times as actuated by rotational speed. Results show good agreement between the observed and the calculated burst frequencies (see below).

It is very important to realize that the valves we mentioned thus far constitute liquid barriers and that they are not barriers for vapors. Vapor barriers must be implemented in any fluidic platform where reagents need to be stored for long periods of time. This is especially important for a disposable diagnostic assay platform. A multi-month, perhaps multi-year, shelf life would require vapor locks to prevent reagent solutions from drying or liquid evaporation and condensation in undesirable areas of the fluidic pathway. Tecan Boston investigated vapor-resistant valves made of wax that was melted to actuate valve opening (G.J. Kellogg, personal communication).

Volume definition (metering) and common distribution channels. The CD centrifugal microfluidic platform enables very fine volume control (or metering) of liquids. Precise volume definition is one of the important functions, necessary in many analytical sample processing protocols, that has been added, for example, to the fluidic design in the Gyrolab MALDI SP1 CD (20). In this CD, developed for matrix assisted laser desorption ionization (MALDI) sample preparation, a common distribution channel feeds several parallel individual sample preparation fluidic structures (**Figure 4**). Reagents are introduced by the capillary force exerted by the hydrophilic surfaces into the common channel and defined volume (200 nl) chambers until a hydrophobic valve stops the flow. When all of the defined volume chambers are filled,

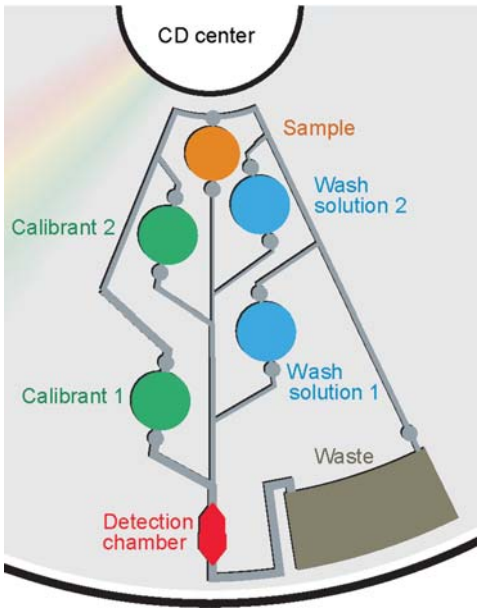

Figure 3

Schematic illustration of the microfluidic structure employed for the ion selective optode CD platform. The fluidic structure contains five solution reservoirs, a detection chamber, and a waste reservoir. The reservoirs contain the first and second calibrant, wash solutions, and the sample. Upon increasing rotation rates, calibrant 1, wash 1, calibrant 2, rinse 2, and then sample were serially gated into the optical detection chamber. Absorption of the calibrants and sample was measured.

the CD is spun at a velocity large enough to move the excess liquid from the common channel into the waste. Although there is sufficient centripetal force to empty the common channel, the velocity is not so high as to allow liquid to move past the hydrophobic valve and the well-defined volume chambers remain filled. These precisely defined volumes can be introduced into the subsequent fluidic structures by increasing the CD angular momentum until the centripetal force allows the liquid to move past the hydrophobic barriers.

Packed columns. Many commercial products are now available that use conventional centrifuges to move liquid, in a controlled manner, through a chromatographic column. One example is the Quick Spin™ protein desalting column (Roche Diagnostics Corp, Indianapolis, IN), based on the size exclusion principle. There is an obvious fit for this same type of separation experiment to be carried out on a CD fluidic device (we sometimes refer to the CD platform as a smart, miniaturized centrifuge). Affinity chromatography has been implemented in the fluidic design of the Gyrolab MALDI SP1 CD (20). A reverse phase chromatography column material (SOURCE™15 RPC) is packed in a microfluidic channel and protein is adsorbed on the column from an aqueous sample as it passes through the column under

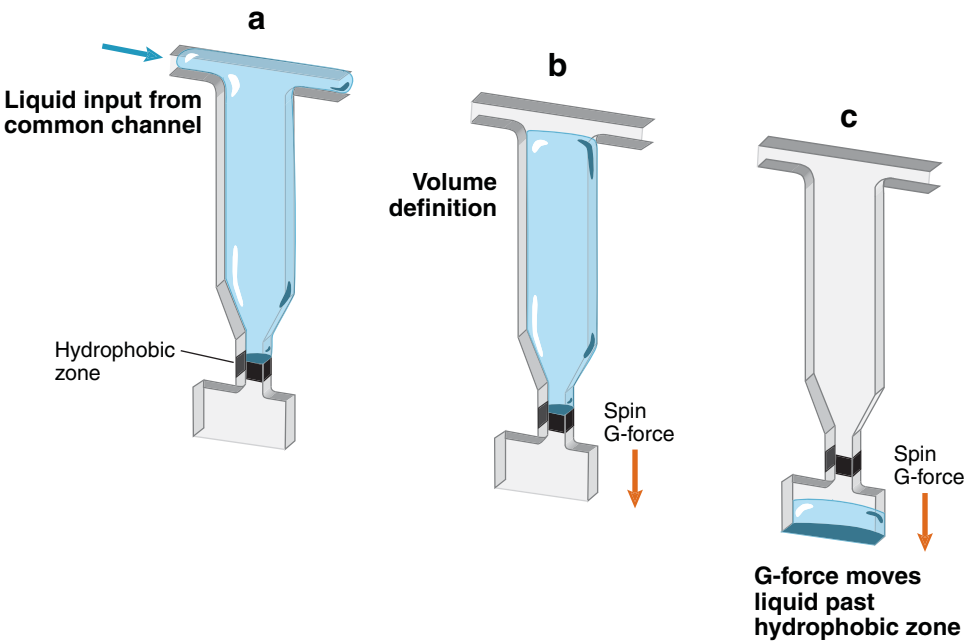

Figure 4

Schematic illustration of liquid metering. (*a*) The common distribution channel and liquid metering reservoirs are filled (by capillary forces) with a reagent to be metered. Liquid entering the reservoir does not pass the hydrophobic zone (valve) because of surface tension forces. (*b*) The CD is rotated at a rate that supplies enough centripetal force to empty the common distribution but not enough to force the liquid through the hydrophobic zone. The volume of the fluid metered is determined by the volume of the reservoir. (*c*) A further increase in the rotational speed provides enough force to move the well-defined volume of solution past the hydrophobic valve. (Figure used with kind permission, Reference 20).

centrifugally controlled flow rates. A rinse solution is subsequently passed through the column, and finally an elution buffer is flowed through to remove the protein and carry it into the fluidic system for further processing. The complete Gyrolab MALDI SP1 CD is discussed in a later section of this review.

CD APPLICATIONS

A CD-based system with ion-selective optode detection and a two-point-calibration structure for the accurate detection of a wide variety of ions was developed (15, 17, 18). Ion-selective optode membranes, composed of plasticized poly(vinyl chloride) impregnated with an ionophore, a chromoionophore, and a lipophilic anionic additive were cast, with a spin-on device, onto a support layer and then immobilized on the disc. With this system, it is possible to deliver calibrant solutions, washing buffers, and "unknown" solutions (e.g., saliva, blood, urine, etc.) to the measuring chamber where the optode membrane is located. This work was further extended to

include anion-selective optodes and fluorescence rather than absorbance detection (17).

The automation of immunoassays on microfluidic platforms presents multiple challenges because of the high number of fluidic processes and the many different liquid reagents involved. Recently, Lai et al. (21) have implemented an automated enzyme-linked immunosorbant assay on the CD platform. Using capillary valving techniques, the sample and reagents were pumped, one at a time, through the detection chamber. Endpoint measurements (completion of enzyme-substrate reaction) were made and compared with conventional microtiter plate methods using similar protocols.

The ability to obtain simultaneous and identical flow rates, incubation times, mixing dynamics, and detection makes the CD an attractive platform for multiple parallel assays. Duffy et al. (10) have reported on a CD system that performs multiple (e.g., 48) enzymatic assays simultaneously by combining centrifugal pumping in microfluidic channels with capillary valving and colorimetric detection. Theophylline, a known inhibitor of the reaction, was used as the model inhibitory compound in Duffy and colleagues' (10) feasibility study. The variation in performance between the individual fluidic CD structures was quantified by carrying out the same assay 45 times simultaneously on a CD. A dose response was seen over 3 orders of magnitude of theophylline concentration in the range of 0.1 mM to 100 mM.

Cell-based assays are often used in drug screening (26) and rely on labor-intensive microtiter plate technologies. Microtiter plate methods may be difficult to automate without the use of large and expensive liquid handling systems, and they present problems with evaporation when scaled down to small volumes. Thomas et al. (23) have reported on a CD platform-based automated adherent cell system (**Figures 5** and **6**). These adherent cell assays involved introducing the compounds to be screened to a cell culture, then determining if the cells were killed (cell viability assay).

In the same work, the authors reported the results of experiments designed to investigate the effect on cells of using centripetal force to move liquids. The cells tested were shown to be compatible with centripetal forces of at least 600 G, much larger than the 50–100 G needed for filling and emptying cell chambers. Furthermore, it was reported that cells grown in such devices appear to show the same cell morphology as cells grown under standard conditions. In separate work done by our group in collaboration with NASA Ames et al. (J.V. Zoval, R. Boulanger, C. Blackwell, B. Borchers & M. Flynn, manuscript in preparation), the LIVE/DEAD®BacLight™ Bacterial Viability Kit (Molecular Probes, Inc., Eugene, OR) has been integrated to a completely automated process on a CD (**Figure 7**). A typical image obtained in a viability assay is shown in **Figure 8**. The disposable and reusable CD structures, hardware, and software were developed for the LIVE/DEAD assay; the entire platform is seen in **Figure 9**.

Nucleic acid analysis is often facilitated by amplification through the polymerase chain reaction (PCR) and requires substantial sample preparation that, unless automated, is labor extensive. After the initial sample preparation step of cell lysis to release the DNA/RNA, a step must be taken to prevent PCR inhibitors, usually certain proteins, such as hemoglobin, from entering into the PCR thermocyle reaction.

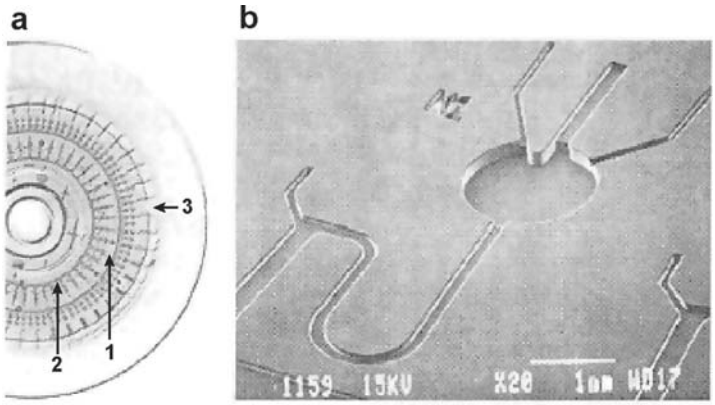

Figure 5

Microfabricated cell culture CD. (*a*) The CD caries a number of cell growth chambers (*1*) radially arranged around a common distribution channel (*2*) and is sealed with a silicone cover (*3*). (*b*) SEM close-up of an individual cell growth chamber and microfluidic connections (reprinted with kind permission from Reference 23).

This can be done by further purification methods, such as precipitation and centrifugation, by solid phase extraction, or by denaturing the inhibitory proteins. Finally, the sample must be mixed with the PCR reagents followed by thermocyling, a process that presents difficulty in a microfluidic environment because of the relatively high temperatures (up to 95°C) required. Kellogg et al. (22) combine sample preparation with PCR on the CD (**Figure 10**). Details of the experimental parameters used can be found in the original reference (22), but to summarize, sample preparation and PCR amplification for two types of samples, whole blood and *Escherichia coli*, were demonstrated on the CD platform and shown to be comparable to conventional methods.

MALDI MS peptide mapping is a commonly used method for protein identification. Correct identification and highly sensitive MS analysis require careful sample

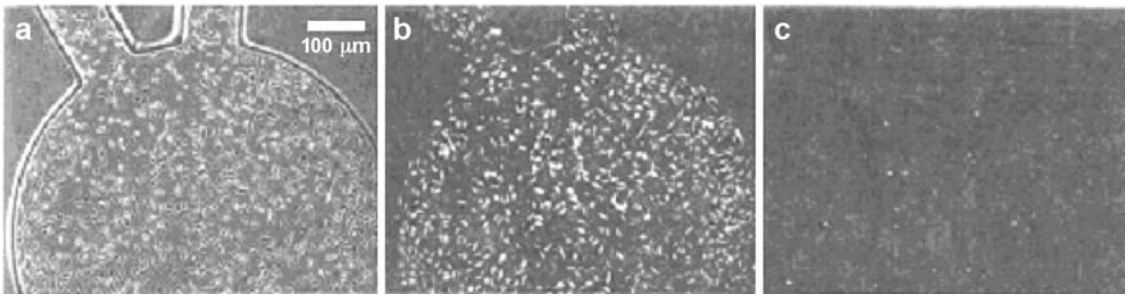

Figure 6

L929 fibroblasts cultured for 48 h in CD growth chambers. (*a*) Phase contrast, (*b*) epifluorescence image of calcein-stained viable cells, (*c*) epifluorescence image of ethidium-stained nonviable cells (reprinted with kind permission from Reference 23).

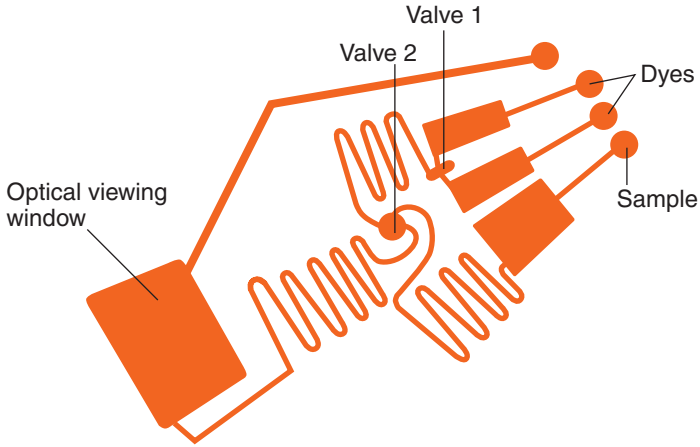

Figure 7

Microfluidic pattern for LIVE/DEAD®BacLight™ Bacterial Viability Assay. The dyes and sample are introduced into the reservoir chambers using a pipette. The dyes fill the chamber stopping at a capillary valve (valve 1). Similarly, the sample containing cells is introduced into the sample reservoir. The disc is rotated to a velocity of 800 rpm, the dyes are forced through the capillary valves, and they are mixed as they flow through the switchback turns of the microfluidic channels. Simultaneously, the sample passes from the reservoir into a fluid channel where it meets the dye mixture at valve 2. The velocity of the disc is increased to 1600 rpm and the dye mixture and sample combine and mix in the switchback microfluidic path leading to the optical viewing window.

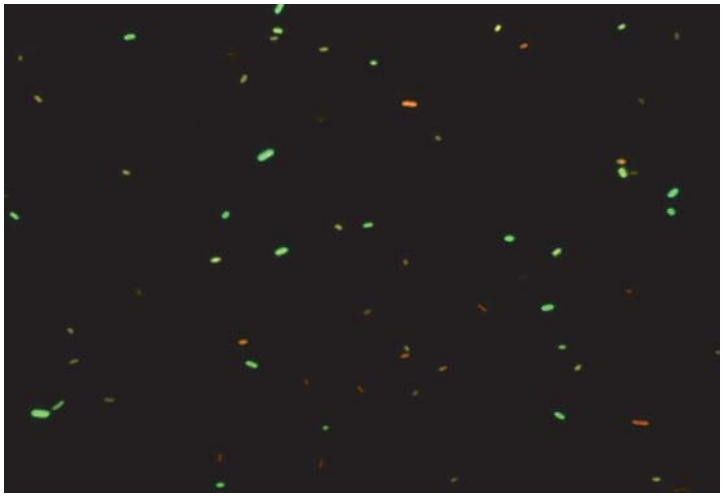

Figure 8

Fluorescent microscopy overlaid images of red- and green-stained *E. coli* on CD from LIVE/DEAD®BacLight™ Bacterial Viability Assay.

Figure 9

Left: Optical disc drive/imager with cover removed. Size of unit is made to fit in specific cargo bay of Space-Lab. Right: Close-up of microscope objectives and a disc loaded in the drive.

preparation. Manual sample preparation is quite tedious and time consuming, and can introduce errors common to multi-step pippetting. MALDI MS sample preparation protocols employ a protein digest followed by sample concentration, purification, and recrystallization with minimal loss of protein. Automation of the sample preparation process, without sample loss or contamination, has been enabled on the CD platform by the Gyrolab MALDI SP1 CD and the Gyrolab Workstation (Gyros AB, Sweden) (20) (**Figure 11**).

The Gyrolab MALDI SP1 sample preparation CD will process up to 96 samples simultaneously using separate microfluidic structures. Gyros reports high reproducibility, high sensitivity, and improved performances when compared with conventional pipette tip technologies.

Microarray Hybridization for Molecular Diagnosis of Infectious Diseases

In recent years, microarrays have become important tools for nucleic acid analysis and gene expression profiling. The expression of thousands of genes can be monitored in a single experiment using this technology. A number of investigators have attempted to adapt this technology to rapidly detect infectious agents in clinical specimens for diagnostic purposes (28–32). However, such systems are still in their infancy and most of them require technologically complex biochips with integrated heating/cooling systems (28, 29, 33). The Madou group at University of California at Irvine, together with the Bergeron group at Laval University, have reported (34) a CD-based microfluidic platform for DNA microarray analysis of infectious disease, presenting an elegant solution to automate and speed up microarray hybridization. *Staphylococcal*-specific oligonucleotides were used as capture probes immobilized in 4×5 arrays of 125 μm spots on a standard 3×1 inch glass slide. The layout of the array is shown in **Figure 12*a***. A flow cell is designed to realize the self-contained hybridization process in the CD platform. As shown in **Figure 12*b***, the flow cell consists of a hybridization

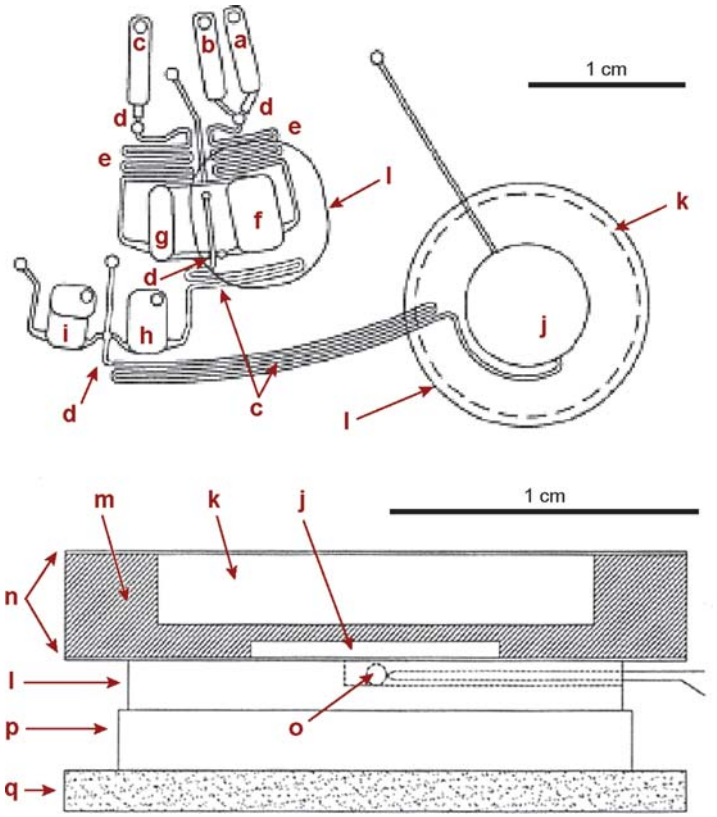

Figure 10

Schematic illustration of the CD microfluidic PCR structure. The center of the disc is above the figure. The elements are (*a*) sample, (*b*) NaOH, (*c*) tris-HCL, (*d*) capillary valves, (*e*) mixing channels, (*f*) lysis chamber, (*g*) tris-HCl holding chamber, (*h*) neutralization lysate holding chamber, (*i*) PCR reagents, (*j*) thermal cycling chamber, and (*k*) air gap. Fluids loaded in (*a*), (*b*), and (*c*) are driven at a first RPM into reservoirs (*g*) and (*f*), at which time (*g*) is heated to 95°C. The RPM is increased and the fluids are driven into (*h*). The RPM is increased and fluids in (*h*) and (*i*) flow into (*j*). On the right, the cross section shows the disc body (*m*), air gap (*k*), sealing layers (*n*), heat sink (*l*), thermoelectric (*p*), PC-board (*q*) and thermistor (*o*) (reprinted with kind permission from Reference 22).

column 1, aligned with the DNA microarray on the glass slide, a sample chamber 2, and rinsing chambers 3 and 4. The reagent chambers are connected to the hybridization column with a microchannel, which is 50 μm in width and 25 μm in depth. The flow cell is aligned with and adhered to the glass slide to form a DNA hybridization detection unit, up to 5 of which can be mounted into the CD platform fabricated from acrylic plastic using CNC machining (**Figure 12*c***). The reagents are positioned to be pumped through the hybridization column by centrifugal force in a sequence beginning with chamber 2 up to chamber 4, and this flow sequence is achieved by manipulating the balance between the capillary force and centrifugal pressure. The

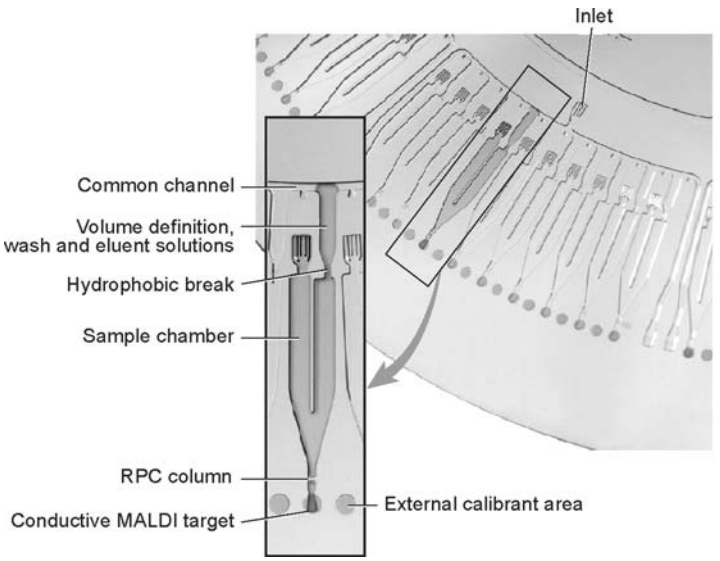

Figure 11

Image of Gyrolab MALDI SP1 sample preparation CD. The protein digest samples are loaded into the sample reservoir (*see inset*) by capillary action. Upon rotation, the sample passes through the RPC column. The peptides are bound to the column and the liquid goes out of the system into the waste. A wash buffer is loaded into the common distribution channel and volume definition chamber. The disc is rotated at an RPM that will empty the common distribution channel but not allow the wash solution to pass through the hydrophobic zone. A further increase of the RPM allows the well-defined volume of wash solution to pass the hydrophobic break and wash the RPC column, then be discarded as waste. Next, a well-defined volume of the elution/matrix solution is loaded and passed through the column, taking the peptides to the MALDI target zone. The flow rate is controlled to optimize the evaporation of the solvent crystallization of the protein and matrix at the target zone (reprinted with kind permission from Reference 20).

sample (chamber 2) is released first and flows over the 140-nl hybridization chamber (chamber 1) where the oligonucleotide capture probes are spotted onto the glass support. The rinsing buffers (chambers 3 and 4) are then released sequentially at a higher angular velocity and are used to wash the nonspecifically bound targets following the hybridization process.

This custom microarray hybridization microfluidic platform is easy to use, automated, and rapid. It uses standard glass slides that are compatible with commercial arrayers and standard commercial scanners found in most academic departments. In this removable microfluidic system, the hybridization chamber is composed of a low-cost elastomeric material, PDMS, using standard moulding methods (35), engrafted with a microfluidic network. This elastomeric material reversibly sticks to the glass slide without any adhesives or chemical reactions, forming the microfluidic unit. Placed onto a plastic CD-like support, the microfluidic units are spun at different speeds to control fluid movements. To simplify hybridization experiments using this device, buffer compositions and capture probe sequences were optimized

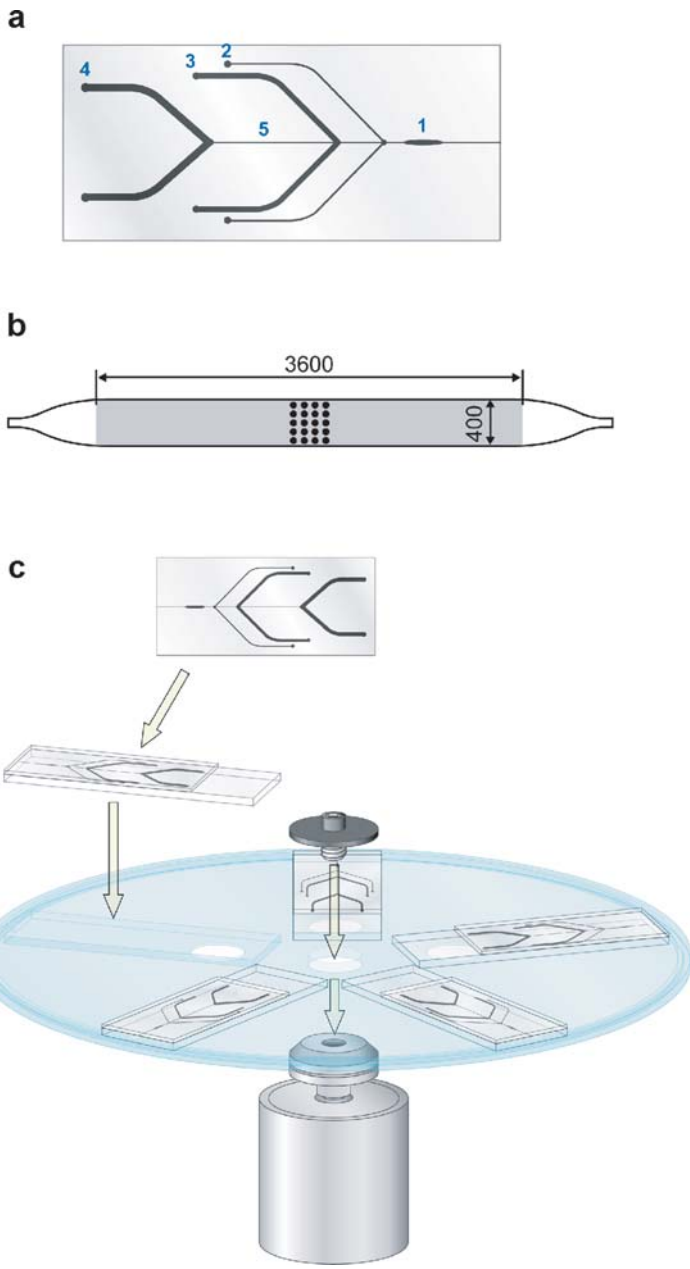

Figure 12

Schematic representation of the microfluidic system. (*a*) PDMS microfluidic unit: The test sample (chamber 2) is released first and flows over the hybridization chamber (chamber 1) where the oligonucleotide capture probes are spotted onto the glass support. The wash buffer in chamber 3 and the rinsing buffer in chamber 4 then start to flow at a higher angular velocity. (*b*) Schematic view of the hybridization chamber showing the dimensions in μm and the area of the chamber (*shaded section*) that can accommodate up to 150 microarray spots. Layout of the *Staphylococcal* microarray used in the present study is also shown (5 capture probes for each species). (*c*) Engraved PDMS is applied to a glass slide on which are arrayed nucleic acid capture probes. The glass slide is placed on a CD support that can hold up to five slides.

to be compatible with room temperature hybridizations to prevent the need for a heating device. Furthermore, this microfluidic system allows a drastic reduction in the volume of reagents needed for microarray hybridizations and does not require a PCR amplicon purification step, which may be time consuming.

In a passive hybridization system, a hybridization event requiring collision between a capture probe and the analyte relies solely on diffusion. In such systems, sensitivity is increased by using longer hybridization periods (36, 37). One advantage of flow through hybridization is that the probability of collision between the probe and the analyte is increased by the much shorter diffusion distance allowed by the shallow hybridization chamber, thereby accelerating the hybridization kinetics (37–39). In the study, it was shown that for the same concentration of 15-mer oligonucleotides or 368 bp amplicons, a 5-min flow-through hybridization increased the kinetics of hybridization, respectively, by a factor of 2.5 and 7.5 in comparison with the passive hybridization. These results are in line with a previous study. Using a microfluidic system, Chung et al. have shown a sixfold rate increase between flow-through hybridization versus passive hybridization. However, this system required a 30-min hybridization step (40). Interestingly, the difference between passive and flow-through hybridization was about three times more important for the amplicons as compared with the shorter 15-mer oligonucleotides (36). This could be explained by the higher diffusion coefficient of the smaller oligonucleotide molecules.

To be used for clinical applications, in addition to being rapid and inexpensive, a molecular test should be sensitive and specific. In 5 min of hybridization, the CD system showed a detection limit of 500 amol of amplified target. This result is comparable with results obtained with more complex microfluidic devices (28, 41). To detect a significant fluorescent signal, an amplification step is required with microarray technology. The CD microfluidic system reported allows detection of amplicons amplified from 10 bacterial genome copies, which is at least 1000 times more sensitive than results obtained by other groups showing microarray hybridization using microfluidic devices (42).

In terms of specificity, the CD system was able to discriminate four different *Staphylococcus* species using a post-PCR hybridization protocol of only 15 min. The *S. aureus* probe, designed with only one mismatch in the *S. epidermidis* amplicon sequence, did not show any significant cross-hybridization. This clearly demonstrates the possibility to discriminate one SNP using the CD system at room temperature and with only 10 μl of washing and rinsing buffer. This SNP discrimination capacity will allow a rapid identification of bacteria and their antibiotic resistance genes.

Cell Lysis on a CD

There are many types of cell lysis methods used today that are based on mechanical (43), physical-chemical (44), chemical (45), and enzymatic (45) principles. The most commonly used methods in biology research labs rely on chemical and enzymatic principles. The main drawbacks of those procedures include intensive labor, adulteration of cell lysate, and the need for additional purification steps. To minimize the required steps for cell lysis, a rapid and reagentless cell lysis method would be

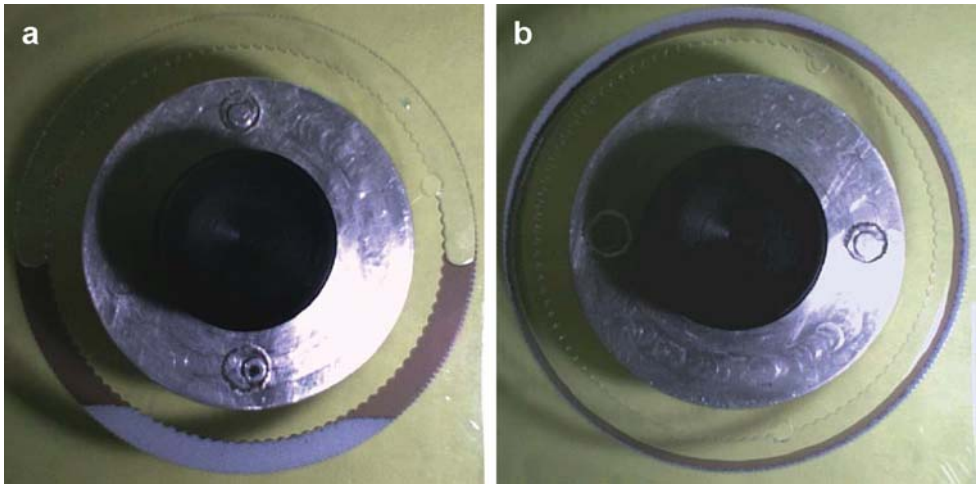

Figure 13

Flow patterns for two rotational states of the CD. (*a*) At rest: beads are sedimented at the bottom of the annular chamber. (*b*) While spinning: two circumferential bands of beads (*lighter*) and liquid (*darker*) are observed.

very useful. Recently, cell lysis has been demonstrated by Kim et al. (46) on a microfluidic CD platform. In this purely mechanical lysis method, spherical particles (beads) in a lysis chamber microfabricated in a CD cause disruption of mammalian (CHO-K1), bacterial (*E. coli*), and yeast (*Saccharomyces cerevisiae*) cells. Investigators took advantage of interactions between beads and cells generated in rimming flow (47, 48) established inside a partially filled annular chamber in the CD rotating around a horizontal axis (**Figure 13**). To maximize bead-cell interactions in the lysis chamber, the CD was spun forward and backward around this axis, using high acceleration for 5 to 7 min. Cell disruption efficiency was verified either through direct microscopic viewing or measurement of the DNA concentration after cell lysing. Lysis efficiency relative to a conventional lysis protocol was approximately 65%. Experiments identified the relative contribution of control parameters such as bead density, angular velocity, acceleration rate, and solid volume fraction.

More recent work (J. Kim, H. Kido, J. Zoval, R. Peytavi, F.J. Picard, et al., manuscript in preparation) by the same investigators used the multiplexed lysis design shown in **Figure 14**. Bead-cell interactions for lysing arise while the beads and cells are pushed back and forth (by switching the CD rotational direction) in the center-tapered lysing chamber. This phenomenon is called the key-stone effect. There are two interaction forces associated with the key-stone effect: collision induced by the geometry and friction owing to relative velocities of beads in motion. The investigators used real-time PCR to characterize the performance of this CD design and achieved 95% lysis efficiency of *B. globigii* spores.

All prototype CDs in this work were fabricated using photolithography and PDMS molding. For the purpose of mechanical cell disruption, an ultrathick SU-8 process

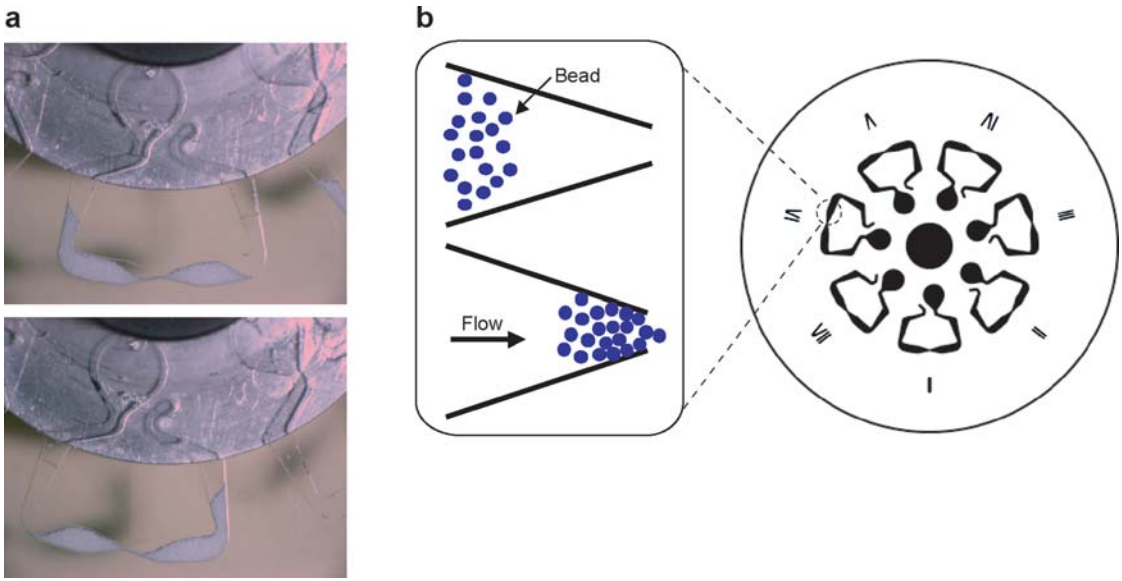

Figure 14

(*a*) Still images of a rotating CD (zirconia-silica beads and water loaded). Top: More beads are observed on the left because of a rapid stop from a clock-wise rotation. Bottom: More beads are on the right because of a rapid stop from a counter clock-wise rotation. (*b*) Diagram of keystone effect.

was developed to fabricate a mold featuring high structures (~1 mm) so that sufficiently high lysing chambers could be formed in the PDMS.

In the long term, this work is geared toward CD-based sample-to-answer nucleic acid analysis, which will include cell lysis, DNA purification, DNA amplification, and DNA hybridization detection.

CD Automated Culture of *C. elegans*

Kim et al. (50) are developing a CD platform for the automated cultivation and gene expression studies of *Caenorhabditis elegans* nematodes. In this research, funded by NASA, the ultimate goal was to understand how a space environment, such as microgravity, hypergravity, and radiation, affects various living creatures. The space environment can cause various physiological changes in organisms that have evolved in unit gravity (1 G) (51). The CD platform is of particular interest in space studies because of its ability to provide a 1 G control using centripetal force; however, its use is not particularly limited to space study applications. A CD capable of the automated culturing of *C. elegans* was developed and is discussed in this section.

The culture system for *C. elegans* contains cultivation chambers, waste chambers, microchannels, and venting holes. Feeding and waste removal processes are achieved automatically using centrifugal force–driven fluidics. In this microfluidic system, the

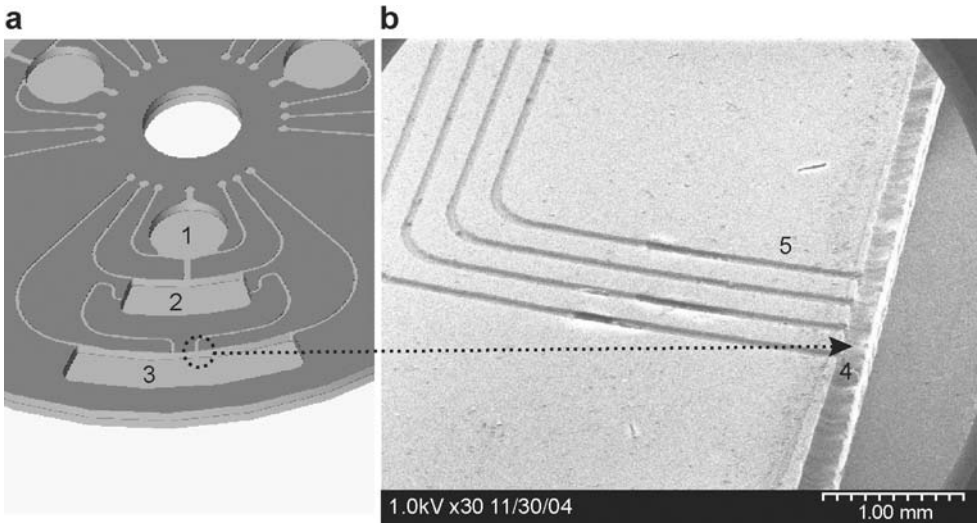

Figure 15

(*a*) Schematic illustration of the microfluidic structure employed for the CD cultivation system. The fluidic structure contains a nutrient reservoir (1), a cultivation chamber (2), and a waste reservoir (3). A liquid nutrient is loaded in a nutrient reservoir (1). Upon increasing the rotation rate of the system, the nutrient solution is gated into the cultivation chamber and some of the waste from the cultivation chamber (150 μl) can drain through the microchannels (50 μm × 40 μm). (*b*) Scanning electron microscopy (SEM) for a cross section of the waste chamber (4), waste removal channels (5) manufactured by photolithography in SU-8. Note that (*a*)-3 is same as (*b*)-4.

nutrient, *E. coli*, and the liquid media are automatically managed for the feeding and waste removal processes. *C. elegans* was selected as a model organism for the gene expression experiment in space owing to its short life span (2–3 weeks), availability of GFP mutants, ease of laboratory cultivation, and completely sequenced genome. Moreover, one can observe its transparent body with a microscope.

The main fabrication material of microfluidic platforms is PDMS, which is highly permeable to gases (a requirement for any aerobic culture), has a chemically inert surface, and is optically transparent down to 300 nm, such that it can be used to observe the behavior of *C. elegans*.

The CD assembly has a two-layer PDMS structure (**Figure 15**) (52). One layer contains the low height channels (40 μm, see **Figure 15*b***) for draining waste from the cultivation chamber, and the other layer contains a cultivation chamber, a loading chamber, and microfluidic connections all with 1 mm heights. This design allows only wastes such as ammonia, not adult worms (80 μm diameter), to be moved from the cultivation chamber to the waste chamber. Cultivation of *C. elegans* was successfully carried out in the CD cultivation system for a period of up to two weeks. *C. elegans* show a specific population growth pattern (**Figure 16**). Based on these results, the Madou group and NASA have begun further development of the CD platform for

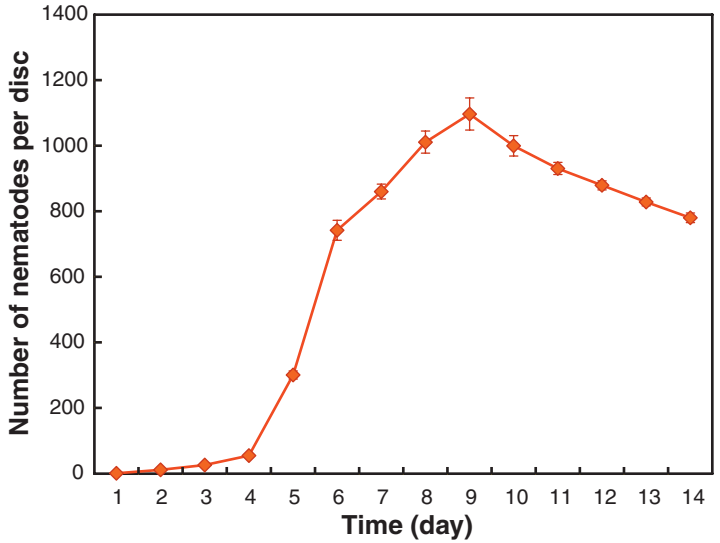

Figure 16

The average number of *C. elegans* cultivated on *E. coli* in liquid medium per cultivation chamber in a CD-based culture under unit gravity (1 G) over a 14-day period. Each day, number of worms per chamber was counted. Values are mean of three replicate experiments ± SEM; three chambers were scored for each experiment.

gene expression experiments to evaluate gene expression changes in *C. elegans* upon exposure to altered gravity conditions and other factors.

CONCLUSION

In comparing miniaturized centrifugal fluidic platforms with other available microfluid propulsion methods, we have demonstrated how CD-based centrifugal methods are advantageous in many analytical situations because of their versatility in handling a wide variety of sample types, ability to gate the flow of liquids (valving), simple rotational motor requirements, ease and economic fabrication methods, and large range of flow rates attainable. Most analytical functions required for a lab-on-a-CD, including metering, dilution, mixing, calibration, separation, etc., have all been successfully demonstrated in the laboratory. Moreover, the possibility of maintaining simultaneous and identical flow rates, to perform identical volume additions, to establish identical incubation times, and to mix dynamics and detection in a multitude of parallel CD assay elements, makes the CD an attractive platform for multiple parallel assays. The platform has been commercialized by Tecan Boston for HTS (4), by Gyros AB for sample preparation techniques for MALDI (20), and by Abaxis (in a somewhat larger and less integrated rotor format compared with the CD format) for human and veterinary diagnostic blood analysis (5). The Abaxis system for human and veterinary medicine uses only dry reagents. But for many diagnostic assays requiring more fluidic steps, there are severe limitations in progressing toward the lab-on-a-CD goal, as liquid storage on the disc becomes necessary. In HTS situations, the CD platform is being coupled to automated liquid reagent loading systems, and no liquids/reagents need to be stored on the disc. The latter made the commercial introduction of the

CD platform for HTS somewhat simpler (4, 20). There is an urgent need, though, for the development of methods for long-term reagent storage that incorporate both liquid and vapor barriers to enable the introduction of lab-on-a-CD platforms for a wide variety of fast diagnostic tests. One possible solution to this problem involves the use of lyophilized reagents with common hydration reservoir feeds, but the issue in this situation becomes the speed of the test, as the time required for redissolving the lyophilized reagents is often substantial.

The CD platform is easily adapted to optical detection methods because it is manufactured with high optical quality plastics enabling absorption, fluorescence, and microscopy techniques. Additionally, the technology developed by the optical disc industry is being used to image the CD at the micron resolution, and the move to DVD and HD DVD will allow submicron resolution. The latter evolution will continue to open up new applications for the CD-based fluid platform. Whereas today the CD fluidic platform may be considered a smart microcentrifuge, we believe that in the future the integration of fluidics and informatics on DVD and HD DVD may lead to a merging of informatics and fluidics on the same disc. One can then envision making very sharp images of the bacteria under test and correlate both test and images with library data on the disc.

ACKNOWLEDGMENT

The authors thank Sue Cresswell (Gyros AB); Gregory J. Kellogg (Tecan Boston); Raj Barathur (Burstein Technologies); Jim Lee (Ohio State University); John Hines, Tony Ricco, and Michael Flynn (NASA Ames); Sylvia Danuert (University of Kentucky); and Regis Peytavi, Dominic Gagné, Francious J. Picard, and Michel G. Bergeron (Laval University).

LITERATURE CITED

1. ALPHA-MOS. **http://www.alpha-mos.com/newframe.htm**
2. Manz A, Verpoorte E, Effenhauser CS, Burggraf N, Raymond DE, et al. 1993. Miniaturization of separation techniques using planar chip technology. *J. High Resolut. Chromatogr.* 16:433–36
3. Caliper. **http://www.calipertech.com**
4. Tecan-Boston Home Page. Look for LabCD-ADMET system. **http://www.tecan-us.com/us-index.htm**
5. Abaxis. **http://www.abaxis.com**
6. Madou MJ. 2002. *Fundamentals of Microfabrication*. Boca Raton, London, New York, Washington DC: CRC Press. 2nd ed.
7. Miyazaki S, Kawai T, Araragi M. 1991. A piezo-electric pump driven by a flexural progressive wave. *Proc. IEEE Micro Electro Mech. Syst. (MEMS '91), Nara, Japan*, pp. 283–88
8. Jorgenson JW, Guthrie EJ. 1983. Liquid chromatography in open-tubular columns. *J. Chromatogr.* 255:335–48

9. Harrison DJ, Fan Z, Fluri K, Seiler K. 1994. Integrated electrophoresis systems for biochemical analyses. *Solid State Sensor and Actuator Workshop*, Hilton Head Island, pp. 21–24
10. Duffy DC, Gills HL, Lin J, Sheppard NF, Kellogg GJ. 1999. Microfabicated centrifugal microfluidic systems: characterization and multiple enzymatic assays. *Anal. Chem*. 71(20):4669–78
11. Madou MJ, Kellogg GJ. 1998. The LabCD^{TM}: a centrifuge-based microfluidic platform for diagnostics. In *Systems and Technologies for Clinical Diagnostics and Drug Discovery*, ed. GE Cohn, A Katzir, 3259:80–93. San Jose, CA:SPIE
12. Kovacs GTA. 1998. Microfluidic devices. In *Micromachined Transducers Sourcebook*, Chap. 9, pp. 787–93. Boston:WCB/McGraw-Hill
13. Ekstrand G, Holmquist C, Örlefors AE, Hellman B, Larsson A, Anderson P. 2000. Microfluidics in a rotating CD. See Ref. 53, pp. 311–14
14. Tiensuu AL, Öhman O, Lundbladh L, Larsson O. 2000. Hydrophobic valves by ink-jet printing on plastic CDs with integrated microfluidics. See Ref. 53, pp. 575–78
15. Madou MJ, Lu Y, Lai S, Lee J, Daunert S. 2000. A centrifugal microfluidic platform—a comparison. See Ref. 53, pp. 565–70
16. Zeng J, Banerjee D, Deshpande M, Gilbert JR, Duffy DC, Kellogg GJ. 2000. Design analysis of capillary burst valves in centrifugal microfluidics. See Ref. 53, pp. 579–82
17. Badr IHA, Johnson RD, Madou MJ, Bachas LG. 2002. Fluorescent ion-selective optode membranes incorporated onto a centrifugal microfluidics platform. *Anal. Chem*. 74(21):5569–75
18. Johnson RD, Badr IHA, Barrett G, Lai S, Lu Y, et al. 2001. Development of a fully integrated analysis system for ions based on ion-selective optodes and centrifugal microfluidics. *Anal. Chem*. 73(16):3940–46
19. McNeely M, Spute M, Tusneem N, Oliphant A. 1999. Hydrophobic microfluidics. *Proc. Microfluidic Devices Syst*. 3877:210–220
20. Gyros AB. *Appl. Rep. 101*, Gyrolab MALDA SP1, Uppsala, Swed.
21. Lai S, Wang S, Luo J, Lee J, Yang S, Madou MJ. 2004. Design of a compact disk-like microfluidic platform for enzyme-linked immunosorbent assay. *Anal. Chem*. 76(7):1832–37
22. Kellogg GJ, Arnold TE, Carvalho BL, Duffy DC, Sheppard NF. 2000. Centrifugal microfluidics: applications. See Ref. 53, pp. 239–42
23. Thomas N, Ocklind A, Blikstad I, Griffiths S, Kenrick M, et al. 2000. Integrated cell based assays in microfabricated disposable CD devices. See Ref. 53, pp. 249–52
24. Anderson AW. 1960. *Physical Chemistry of Surfaces*, pp. 5–6. New York, London, Sidney: Wiley
25. Deleted in proof
26. Burbaum J. 1998. Miniaturization technologies in HTS: how fast, how small, how soon? *Drug Discov. Today* 3(7):313–22
27. Deleted in proof

28. Wang Y, Vaidya B, Farquar HD, Stryjewski W, Hammer RP, et al. 2003. Microarrays assembled in microfluidic chips fabricated from poly(methyl methacrylate) for the detection of low-abundant DNA mutations. *Anal. Chem.* 75:1130–40
29. Mikhailovich V, Lapa S, Gryadunov D, Sobolev A, Strizhkov B, et al. 2001. Identification of rifampin-resistant *Mycobacterium tuberculosis* strains by hybridization, PCR, and ligase detection reaction on oligonucleotide microchips. *J. Clin. Microbiol.* 39:2531–40
30. Bekal S, Brousseau R, Masson L, Prefontaine G, Fairbrother J, Harel J. 2003. Rapid identification of *Escherichia coli* pathotypes by virulence gene detection with DNA microarrays. *J. Clin. Microbiol*. 41:2113–25
31. Bavykin SG, Akowski JP, Zakhariev VM, Barsky VE, Perov AN, Mirzabekov AD. 2001. Portable system for microbial sample preparation and oligonucleotide microarray analysis. *Appl. Environ. Microbiol*. 67:922–28
32. Westin L, Miller C, Vollmer D, Canter D, Radtkey R, et al. 2001. Antimicrobial resistance and bacterial identification utilizing a microelectronic chip array. *J. Clin. Microbiol.* 39:1097–104
33. Fan HZ, Mangru S, Granzow R, Heaney P, Ho W, et al. 1999. Dynamic DNA hybridization on a chip using paramagnetic beads. *Anal. Chem.* 71:4851–59
34. Peytavi R, Raymond FR, Boissinot K, Picard FJ, Boissinot M, et al. 2005. *Anal. Chem.* Submitted
35. Duffy DC, McDonald JC, Schueller OJA, Whitesides GM. 1998. Rapid prototyping of microfluidic systems in poly(dimethylsiloxane). *Anal. Chem*. 70:4974–84
36. Chan V, Graves DJ, McKenzie SE. 1995. The biophysics of DNA hybridization with immobilized oligonucleotide probes. *Biophys. J.* 69:2243–55
37. McQuain MK, Seale K, Peek J, Fisher TS, Levy S, et al. 2004. Chaotic mixer improves microarray hybridization. *Anal. Biochem.* 325:215–26
38. Bringuier E, Bourdon A. 2003. Colloid transport in nonuniform temperature. *Phys. Rev. E Stat. Nonlin. Soft Matter Phys*. 67:011404
39. Axelrod D, Wang MD. 1994. Reduction-of-dimensionality kinetics at reaction-limited cell-surface receptors. *Biophys. J.* 66:588–600
40. Chung YC, Lin YC, Shiu MZ, Chang WN. 2003. Microfluidic chip for fast nucleic acid hybridization. *Lab Chip* 3:228–33
41. Liu RH, Lenigk R, Druyor-Sanchez RL, Yang J, Grodzinski P. 2003. Hybridization enhancement using cavitation microstreaming. *Anal. Chem*. 75:1911–17
42. Lenigk R, Liu RH, Athavale M, Chen Z, Ganser D, et al. 2002. Plastic biochannel hybridization devices: a new concept for microfluidic DNA arrays. *Anal. Biochem.* 311:40–49
43. Carlo DD, Jeong KH, Lee LP. 2003. Reagentless mechanical cell lysis by nanoscale barbs in microchannels for sample preparation. *Lab Chip* 3:287–91
44. Lee SW, Tai YC. 1999. A micro cell lysis device. *Sens. Actuators A* 73:74–79
45. Sambrook J, Russell DW. 2001. *Molecular Cloning*. Cold Spring Harbor, NY: Cold Spring Harbor Lab. Press
46. Kim J, Jang SH, Jia G, Zoval JV, Da Silva NA, Madou MJ. 2004. Cell lysis on a microfluidic CD (compact disc). *Lab Chip* 4:516–22
47. Ruschak KJ, Scriven LE. 1976. Rimming flow of liquid in a rotating horizontal cylinder. *J. Fluid Mech*. 76:113–25

48. Thoroddsen ST, Mahadevan L. 1997. Experimental study of coating flows in a partially-filled horizontally rotating cylinder. *Exp. Fluids* 23:1–13
49. Deleted in proof
50. Kim N, Dempsey CM, Zoval JV, Sze JY, Madou MJ. 2006. Automated microfluidic compact disc (CD) cultivation system of *C. elegans*. Submitted
51. Le Bourg E. 1999. A review of the effects of microgravity and of hypergravity on aging and longevity. *Exp. Gerontol.* 34:319–36
52. Wu H, Odom TW, Chiu DT, Whitesides GM. 2003. Fabrication of complex three-dimensional microchannel systems in PDMS. *J. Am. Chem. Soc.* 125:554–59
53. van den Berg A, Olthuis W, Bergveld P. 2000. *Micro Total Analysis Systems 2000*. Dordrecht: Kluwer Acad.

Annual Review
of Biomedical
Engineering

Volume 8, 2006

Contents